

# Fabrication of Novel Silicone Capsules with Tunable Mechanical Properties by Microfluidic Techniques

Neus Vilanova,<sup>†,‡</sup> Carlos Rodríguez-Abreu,<sup>\*,§</sup> Alberto Fernández-Nieves,<sup>‡</sup> and Conxita Solans<sup>†</sup>

<sup>†</sup>Institute for Advanced Chemistry of Catalonia, Consejo Superior de Investigaciones Científicas (IQAC–CSIC) and CIBER de Bioingeniería, Biomateriales y Nanomedicina (CIBER-BBN), Barcelona, Spain

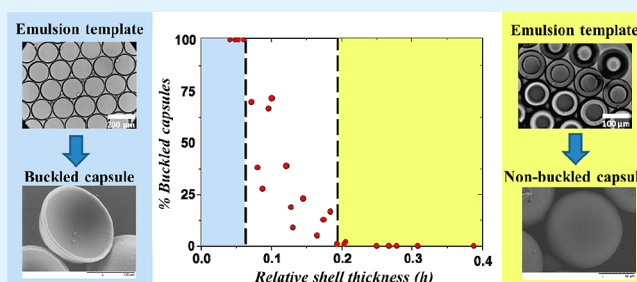
<sup>‡</sup>Soft Condensed Matter Laboratory, School of Physics, Georgia Institute of Technology, Atlanta, Georgia, United States

<sup>§</sup>International Iberian Nanotechnology Laboratory (INL), Braga, Portugal

## S Supporting Information

**ABSTRACT:** A novel approach for the synthesis of silicone capsules using double W/O/W emulsions as templates is introduced. The low viscosity of the silicone precursors enables the use of microfluidic techniques to accurately control the size and morphology of the double emulsion droplets, which after cross-linking result in the desired monodisperse silicone capsules. Their shell thickness can be finely tuned, which in turn allows control over their permeability and mechanical properties; the latter are particularly important in a variety of practical applications where the capsules are subjected to large external forces. The potential of these capsules for controlled release is also demonstrated using a model hydrophilic substance.

**KEYWORDS:** microfluidic, silicone, capsules, buckled, elasticity, release



## INTRODUCTION

Microcapsules are employed in a wide range of applications, from agrochemical to biomedical and from cosmetics to material science. Among all materials that can be used to prepare microcapsules, silicones are particularly attractive. Silicones are organosilicon compounds made of [SiRR'O] repeating units, where R and R' are side groups that can be reactive. Poly(dimethylsiloxane) is the major building block of many silicone materials. Moreover, when a cross-linking reaction takes place between these reactive groups, a three-dimensional silicone network is formed. Cross-linked silicones have interesting properties such as low glass transition temperatures, thermal and chemical stability, good resistance to light, high permeability to various organic solvents and gases, high hydrophobicity, low density, and biocompatibility.<sup>1,2</sup> All of them mainly arise from the strength and the nature of the Si–O bond, the low intermolecular interactions and the chemical characteristics of the side groups. In addition, the elastic properties of cross-linked silicones can be easily tuned by controlling either the structure or the degree of cross-linking of the network.<sup>3,4</sup> It is this extensive set of interesting properties shared by all silicone materials that makes them attractive in a variety of fields, for example as gas-separation membranes,<sup>5</sup> as coatings to impart desired surface properties such as hydrophobicity,<sup>6,7</sup> as metamaterials in acoustics,<sup>8</sup> or in biomedical applications,<sup>9,10</sup> where they are processed in a wide range of formats. However, the generation of silicone particles or capsules by bulk emulsification techniques has proved to be

challenging<sup>11,12</sup> and in general results in a lack of an accurate control over the final properties of the particles, typically because of limitations in the emulsification process.<sup>13,14</sup> Therefore, there is a demand for new innovative approaches. In this regard, microfluidic techniques arise as a novel strategy because the precise manipulation of liquid phases allows the formation of monodisperse droplets and particles with a well-defined morphology, structure, and composition. However, despite the great advantages of these techniques, the synthesis of silicone particles with such technologies is still not so extended;<sup>15</sup> reports on their use for generating capsules are also scarce,<sup>16</sup> as the high viscosity of the most common cross-linkable silicones and their long cross-linking times hamper their manipulation inside the microfluidic devices.<sup>4,15,17</sup>

To overcome these drawbacks, we used thermally cross-linkable silicones with low molecular weights and therefore low viscosities to fabricate, for the first time, poly(dimethylsiloxane) capsules in glass-based microfluidic devices via double emulsion templating. First, we discuss the formation of monodisperse double W/O/W emulsions, with a mixture of cross-linkable silicones as the oil phase. Then we show how these double emulsions are used as templates to create silicone capsules for encapsulation and controlled release applications.

Received: March 26, 2013

Accepted: May 9, 2013

Published: May 9, 2013

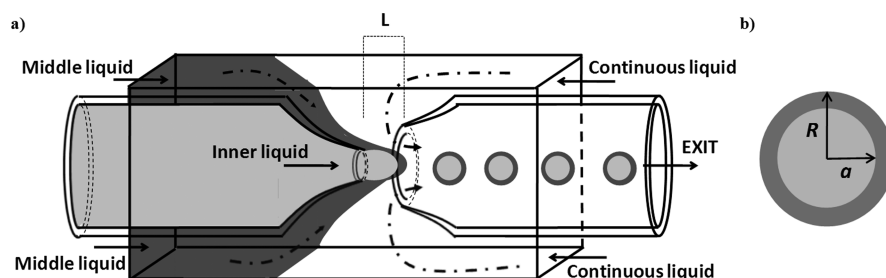


**Figure 1.** (a) Illustration of the microfluidic device used to create double emulsions and (b) geometric parameters used to characterize the resulting double emulsion droplets.

## EXPERIMENTAL SECTION

**Materials.** The cross-linkable vinyl dimethylsiloxy-terminated polydimethylsiloxane (designated as PDMS) with a kinematic viscosity of  $\nu = 0.7$  cSt (MW = 186 g/mol) was obtained from ABCR (Germany). The cross-linker trimethylsilyl-terminated poly(dimethylsiloxane-co-methyl hydrosiloxane) containing 50% mol of methylhydrosiloxane and with  $\nu = 12$  cSt (MW = 950 g/mol) was supplied by Sigma-Aldrich (USA). The hydrophobic surfactant KF-6104 (HLB = 3–4) was obtained as a gift from Shin-Etsu (Japan). The surfactant is a polyglyceryl-3-polydimethylsiloxyethyl dimethicone, namely, a branched dimethicone copolymer with polyglycerine groups. A platinum (0)-1,3-divinyl-1,1,3,3-tetramethyl-disiloxane complex, obtained from Sigma-Aldrich (USA), was used as a cross-linking catalyst dissolved in chloroform at a concentration of 9.7 wt %. The hydrophilic surfactant Tween 80, a poly(oxyethylene) sorbitol ester with 20 oxyethylene units, was supplied by Merck (Germany). Finally, the hydrophilic sodium fluorescein (Sigma-Aldrich, USA) was employed as a model molecule in the encapsulation experiments and NaCl (Sigma-Aldrich, USA) to balance the osmotic pressure difference between the inner phase of the double emulsion droplets and the continuous phase. All chemicals were used as received. Milli-Q water with a conductivity of  $18.2 \text{ M}\Omega \text{ cm}^{-1}$  was used in all experiments.

**Fabrication of Silicone Double Emulsions.** A microfluidic device that combines coflow and flow-focusing<sup>18</sup> was used to produce monodisperse silicone double W/O/W emulsions. It consisted of three glass capillaries. One of them had a square cross-section and contained the other two, which were cylindrical, coaxially aligned and previously pulled to a desired tip diameter. They were facing each other at a tip-to-tip distance  $L$ , as shown in Figure 1a. Typical tip diameters were within the range of 25–250  $\mu\text{m}$  and  $L$  was varied but always kept smaller than the larger of the two tip diameters,  $D_{\text{tip}}$ . The inner and middle liquids were pumped through the cylindrical capillary with the smallest tip and through the voids between the square and circular cross-section of the corresponding outer and cylindrical capillaries, as shown in Figure 1a. The continuous liquid was pumped in the opposite direction through the voids left between the same outer capillary and the other cylindrical capillary, as also shown in Figure 1a. In this way, this liquid hydrodynamically focused the coaxial flow of the other two through this second cylindrical capillary, which provided the exit of the device and served to collect the double emulsion droplets.

The composition of the different liquid phases is indicated in Table 1. The polymer mixture was composed of the PDMS and the cross-linker at a weight ratio of 30/70. Prior to their injection in the microfluidic device, all solutions were filtered through a membrane with a pore size of 1  $\mu\text{m}$ . Flow rates of all liquids were adjusted to establish the conditions for a controllable generation of the double W/O/W droplets in the dripping regime.<sup>19</sup> Their formation was monitored using a high speed camera (Vision Research, Phantom v9.1) coupled to an inverted optical microscope (Carl Zeiss, Axio-observer A1).

**Fabrication of Silicone Capsules.** Capsules were obtained after cross-linking the middle oil phase of the W/O/W double emulsion droplets. This was done by heating them outside the device to prevent clogging of the capillaries. The general procedure consisted of

**Table 1. Composition of the Various Liquids Used to Produce the Double W/O/W Emulsions**

|                       | components             | wt % |
|-----------------------|------------------------|------|
| inner liquid (W)      | water                  | 100  |
| middle liquid (O)     | polymer mixture        | 70.2 |
|                       | hydrophobic surfactant | 17.5 |
|                       | catalyst solution      | 12.3 |
| continuous liquid (W) | hydrophilic surfactant | 5    |
|                       | water                  | 95   |

collecting the double emulsions in a hot water bath at  $\sim 70$  °C; this initiates the cross-linking reaction. Normally, the droplets were maintained at this temperature for 15 min, which was enough time for the formation of the desired solid shell. Subsequently, the capsule suspension was filtered through a membrane with a pore size of 2  $\mu\text{m}$ . Then, the capsules were washed with acetone and dried at 60 °C for 24 h; this last step also helped to complete the cross-linking reaction. Capsules were imaged by optical microscopy and scanning electron microscopy (SEM, Hitachi TM-1000). The relative thickness is defined as  $h = [R - a]/R$ , where  $R$  and  $a$  are the outer and inner radii of the shell, respectively (see Figure 1b). At least 100 capsules were used to obtain statistically meaningful values of  $h$ . Because in some cases buckling of the capsules was observed, their fraction was determined from the number of buckled capsules divided by the total number of capsules counted.

**Determination of Mechanical Properties of Silicone Monoliths.** For the measurement of mechanical properties of the silicone matrix, poly(dimethylsiloxane) monoliths (diameter = 14 mm; thickness = 12 mm) were prepared. The precursor solutions of such monoliths had the same composition as the middle liquid in emulsions and were cross-linked following the same procedure described for capsules. The elastic modulus was determined by performing compression assays using a MT-LQ dynamometer (Stable Micro-Systems). Measurements were performed at a crosshead speed of 0.2 mm/s until an indentation displacement of 4 mm. The elastic moduli were calculated from the linear zone of the loading curve.

**Release Experiments.** To study the release of fluorescein from the capsules, we fixed 5 mg of previously loaded capsules to a double-sided tape stuck to the bottom of a spectrophotometer cuvette and 3 mL of the receptor solvent were added. The cuvette was kept at 25 °C without stirring. The spectrum of the receptor solution was then measured at different times using a UV-Vis spectrophotometer (Cary300, Varian) and the amount of released fluorescein was determined from a previously determined calibration curve. The amount of encapsulated fluorescein was obtained from a spectrum after crashing and dispersing in water some of the original loaded capsules.

## RESULTS

Using the components and methods outlined above, we obtained W/O/W double emulsion droplets with a single internal droplet. The presence of hydrophobic surfactant in the oil phase and hydrophilic surfactant in the continuous aqueous

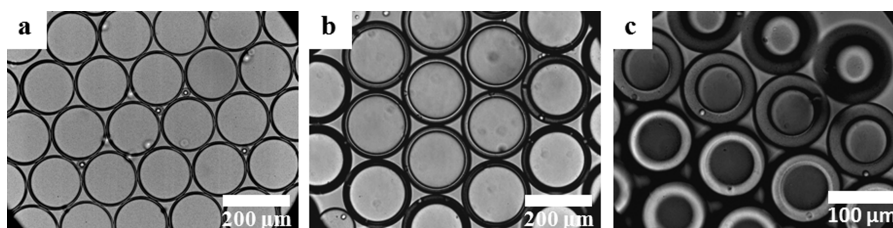


**Figure 2.** Optical micrographs of double emulsion droplets obtained at different flow conditions and with different sizes and relative shell thicknesses ( $h$ ): (a)  $R = 81.5 \pm 0.6 \mu\text{m}$ ,  $h = 0.05 \pm 0.01$ ,  $Q_{\text{ML}}/Q_{\text{IL}} = 0.2$ ,  $Q_{\text{OL}} = 50 \text{ mL/h}$ ; (b)  $R = 102.3 \pm 0.9 \mu\text{m}$ ,  $h = 0.17 \pm 0.02$ ,  $Q_{\text{ML}}/Q_{\text{IL}} = 0.8$ ,  $Q_{\text{OL}} = 25 \text{ mL/h}$ ; and (c)  $R = 57.8 \pm 0.5 \mu\text{m}$ ,  $h = 0.39 \pm 0.02$ ,  $Q_{\text{ML}}/Q_{\text{IL}} = 2.5$ ,  $Q_{\text{OL}} = 15 \text{ mL/h}$ .

phase guaranteed the stability of the droplets against break-up or coalescence.<sup>20</sup> In general, the coefficients of variation for the outer radii  $R$  were  $\sim 1\%$  of the mean, indicating a high monodispersity of the double emulsions droplets. As a result, the droplets assembled into highly ordered hexagonal lattices at sufficiently high concentrations, as shown in Figure 2.

The outer radius was tuned from 30 to more than  $100 \mu\text{m}$  by varying  $D_{\text{tip}}$  and the flow rate of the continuous liquid ( $Q_{\text{OL}}$ ) (see the Supporting Information, Figure S1–S2). The relative shell thickness was also tuned by changing the ratio between the middle and inner liquid flow rates,  $Q_{\text{ML}}/Q_{\text{IL}}$ ; for a given device with a certain  $D_{\text{tip}}$ , the shells were thicker by increasing  $Q_{\text{ML}}/Q_{\text{IL}}$  as exemplified in Figure 3. Such tendency is also

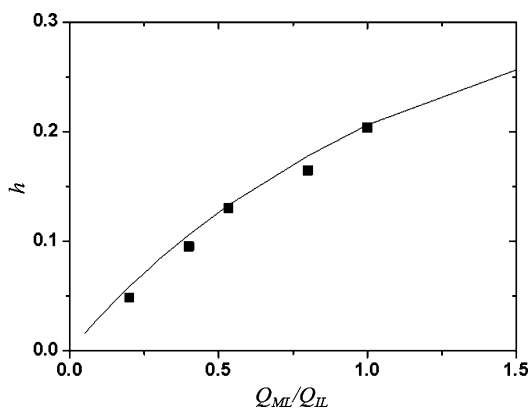


**Figure 3.** Relative shell thickness ( $h$ ) as a function of the ratio between the middle and inner liquid flow rates,  $Q_{\text{ML}}/Q_{\text{IL}}$ , for a given device with  $D_{\text{tip}} = 150 \mu\text{m}$ . The solid line represents predicted values of  $h$  based on the equation  $h = 1 - (1 + Q_{\text{ML}}/Q_{\text{IL}})^{-1/3}$ .<sup>21,22</sup>

described in earlier works by the following mass balance:  $h = 1 - (1 + Q_{\text{ML}}/Q_{\text{IL}})^{-1/3}$ .<sup>21,22</sup> The solid line in Figure 3 shows that the experimental data was consistent with the previous equation. By adjusting the flow rates of different devices, shell thickness could be finely tuned from  $h = 0.05$  (Figure 2a) up to  $h = 0.39$  (Figure 2c).

To fabricate monodisperse silicone capsules, we thermally cross-linked the middle phase of the double emulsion droplets. Figure 4 shows optical and scanning electron micrographs of the capsules obtained from the double emulsions shown in Figure 2. Given that there was no need to dissolve the silicone precursors in organic solvents, the middle oily phase was almost totally converted into the cross-linked silicone network. This is supported by the fact that the resulting capsules were replicas of the double emulsion templates; only a very small shrinkage in  $R$ ,  $\sim 1.5\%$  of the original emulsion size, was observed. As expected, the opacity of the capsules in the optical microscopy images increases with increasing shell thickness, as shown in

Figures 4a–c. In addition, SEM images show that while the thinnest capsules have a nonporous shell (Figure 4d), thicker capsules have increasingly larger pores (Figure 4e, f). This could result from the presence of chloroform in the catalyst solution. Although for thin shells the amount of chloroform is small and could evaporate quickly, for thicker shells the larger amount used could result in longer evaporation times; in these cases, the chloroform may act as porogen during the formation of the polymer network.

Among the dried capsules, there were some that were irreversibly buckled (Figure 4a, d) and some which retained their spherical shape (Figure 4c, f). The determining parameter controlling this behavior is the relative shell thickness  $h$  (parameter that combines both  $a$  and  $R$ ). It was found that for  $h \geq 0.19$ , all capsules were stiff enough to retain their spherical shape after drying, while for  $h \leq 0.06$ , all capsules exhibited an irreversible buckling. In between, for  $0.19 \geq h \geq 0.06$ , there was a mixture of both types of capsules (Figures 4b, e). Hence, the transition between the two morphologies was not sharp and the percentage of buckled capsules progressively increased as  $h$  decreased from 0.19 to 0.06, as shown in Figure 5. This could result from differences in the homogeneity of the shell thickness among the capsules, which could be given from a gravity-induced displacement of the inner liquid core in the original double emulsion droplets during the cross-linking reaction.<sup>21</sup> Such gradual transition zone could also be attributed to inhomogeneities and varying conditions along the sample during drying. It is argued that capsules in the transition zone ( $0.06 < h < 0.19$ ) could be more sensitive to such conditions; probably a more precise control of the drying process could lead to a sharper transition. The presence of buckling can be understood with simple elasticity arguments.<sup>23,24</sup> In the present study, the driving force for buckling results from the pressure difference between the inside and outside of the capsule while drying. When this force cannot be compensated by the restoring elastic force of the shell, the spherical capsule loses its shape.<sup>25,26</sup> This critical pressure difference is given by:<sup>27</sup>  $P_c = 4\mu h^2$ , where  $\mu$  is the elastic modulus of the material. This equation suggests that buckling solely depends on  $h$  for a given material, in agreement with the previously described observations (Figure 5).

The elastic modulus also plays a role in this transition. For these silicone capsules,  $\mu$  is determined by the degree of cross-linking; a decrease in the cross-linking degree directly reverts into a decrease in the stiffness of the capsule.<sup>4,28</sup> To test this, double emulsion droplets with  $h \leq 0.06$  were generated and subsequently kept at  $70 \text{ }^\circ\text{C}$  for just 5 min; with this short reaction time the capsules were expected to have a lower cross-linking degree than that of the capsules discussed above. This difference should be further enhanced since the final drying of the fabrication process was performed at room temperature

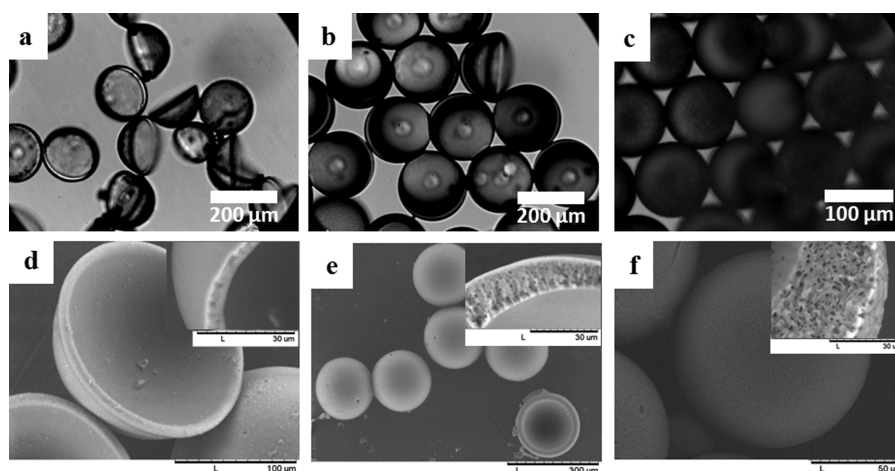


**Figure 4.** (a–c) Optical micrographs of dried capsules produced from the double W/O/W emulsion droplets of Figure 2. (d–f) Scanning electron microscopy images of the same dried capsules. Inset: Details of the shell of broken capsules.

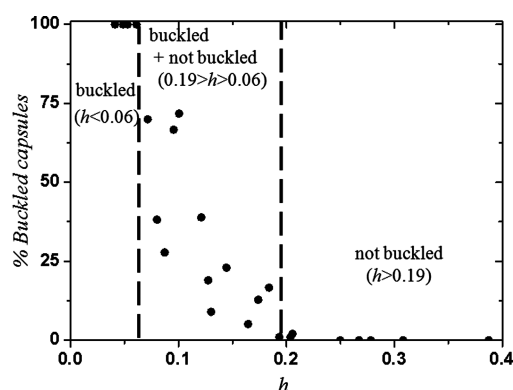


**Figure 5.** Percentage of buckled capsules as a function of  $h$ .

rather than at 60 °C. The resulting capsules buckled and deformed when dried, as shown in Figures 6a–c; which was consistent with the previous results. Interestingly, these capsules recovered their original spherical shape without any evidence of crack or defect formation when resuspended in acetone. This reversibility (not observed with capsules cross-linked for longer times) indicated a very wide elastic regime,

which persisted for deformations even of the order of the capsule diameter. The large deformation of these capsules supports the idea that they are indeed more elastic than those obtained after longer reaction times.

Similarly, to confirm the effect of the cross-linking time on the mechanical properties of the network, silicone monoliths were cross-linked under the same conditions as the capsules. During the compression test, the monolith cured for 15 min collapsed after reaching a deformation of 24% (see Figure S3 in the Supporting Information). Conversely, the monolith cured for only 5 min did not show evidence of fractures after the test, indeed, the unloading curve almost overlapped the loading curve (see Figure S3 in the Supporting Information), which is expected for elastic materials. The obtained elastic moduli were 0.37 and 0.10 MPa for the monoliths cured for 15 and 5 min, respectively. Hence, it is confirmed that the elastic modulus of the material decreases with the cross-linking degree, which effectively allows obtaining elastic silicone networks.

To study the potential of the silicone capsules as encapsulation and release vehicles, double W/O/W emulsion droplets with an inner core containing fluorescein at a concentration of 0.007 M were generated. It is worth noting that the osmolarity of the continuous liquid was matched to

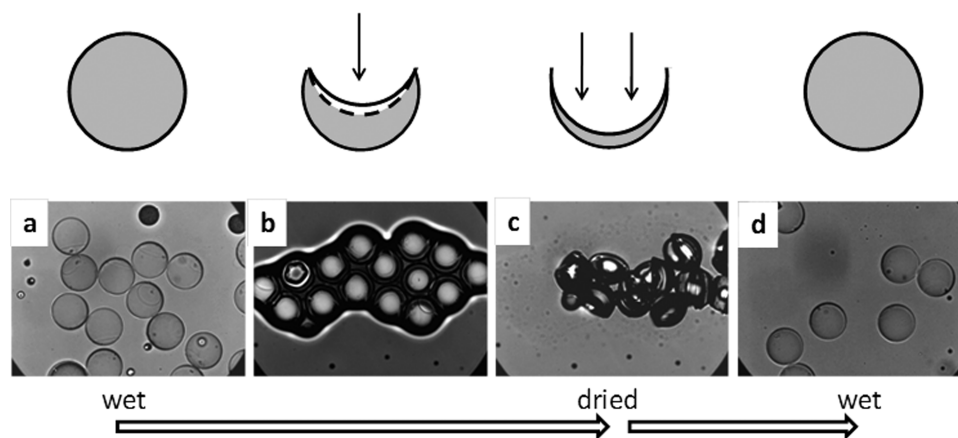


**Figure 6.** Optical micrographs of the evolution of capsules with a low elastic modulus during drying and resuspension. (a–c) The capsules were observed to dramatically buckle, but (d) they were able to completely recover their original spherical shape after resuspension.

that of the inner liquid by adding NaCl to the former, first to avoid fluorescein diffusion due to osmotic pressure differences and second to prevent shell thickness variations during the cross-linking process. During the formation of the emulsion, the contact between both aqueous liquids, inner and continuous, was prevented by the hydrophobic middle liquid. Thus, there was almost no diffusion of the fluorescein from the inner core to the continuous phase, resulting in encapsulation efficiencies of  $\sim 100\%$ . This was confirmed by the lack of fluorescence signal in the continuous phase. Fluorescein remained successfully encapsulated within the liquid core as long as the system was in the liquid state. During shell formation, however, some leakage of fluorescein from the inner droplets was observed, probably due to the formation of pores on the shell as a result of the already mentioned porogen action of the chloroform. Such pores might act as diffusion channels during the reaction time. Moreover, during the washing process some fluorescein was also lost, as the washing liquid (acetone) acts as a swelling agent as commented below. Such leakage led to loading efficiencies for the capsules of around 19–26%. The final encapsulated amount ranged between 0.52 to 1.74 mg of fluorescein per gram of capsules depending on their inner volume.

The release experiments were performed at 25 °C with fluorescein-loaded capsules of different shell thicknesses in contact with water, and the results are presented in Figure 7.

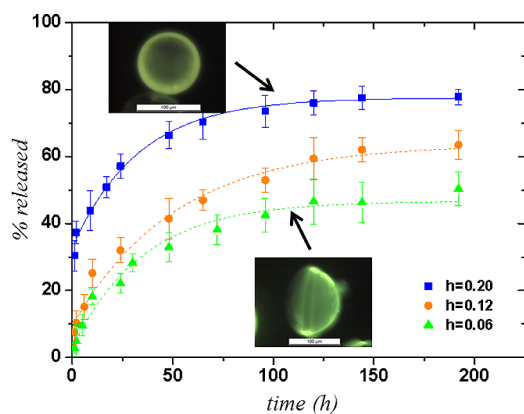


**Figure 7.** Release profiles at 25 °C of fluorescein from capsules in contact with water. The insets are fluorescence optical microscopy images of spherical (up) and buckled (down) loaded capsules. The solid line is a fit to eq 1 in the text. Dashed lines are guides to the eye only.

The fluorescence images in the insets of Figure 7 show that initially the fluorescein was homogeneously distributed over the inner walls of the shells, regardless of their morphology; this ruled out any significant structural differences with the shell. Capsules with relative shell thickness  $h = 0.20$  showed an abrupt initial burst of fluorescein followed by a decrease in the release rate. On the contrary, capsules with relative shell thicknesses  $h = 0.12$  and  $h = 0.06$  showed less dramatic initial bursts and much more gradual release profiles. Presumably, it is the presence of pores in the walls of thicker shells which promoted the initial abrupt burst and facilitated the release of fluorescein, which was otherwise hindered by the presence of the highly nonporous hydrophobic wall. To better understand the experimental data, a model for the release of a substance from a spherical capsule of radius  $R$  and shell thickness  $\delta$  was considered, assuming that the concentration of the encapsu-

lated substance in the core of the capsule changes slowly compared to the characteristic diffusion time through the shell<sup>29</sup>

$$\% \text{released} = (100 - X_0) \left( 1 - \exp \left( - \frac{3D(R + \delta)}{R^2 \delta} t \right) \right) + X_0 \quad (1)$$

Where  $D$  is the diffusion coefficient of the encapsulated substance in the shell and  $X_0$  is the amount of substance released during the initial burst. Since the model assumes a spherical geometry, experimental data for  $h = 0.12$  or  $0.06$  were not fitted to eq 1, as those data correspond to mixtures of spherical and buckled capsules, consequently only the release profile of non-buckled capsules ( $h=0.20$ ) was considered. The model described very well the data of these spherical capsules, as shown by the solid line in Figure 7. From the fit to the data, a diffusion coefficient of  $5.65 \times 10^{-12} \text{ m}^2/\text{h}$  was obtained, which is comparable to that reported in the literature for fluorescein diffusing inside different host matrices.<sup>30</sup>

The release into ethanol for buckled capsules with  $h = 0.06$  was also studied. In this case, the release was significantly faster than in water and was complete after about 2 h, as shown in Figure 8. This is consistent with the expected swelling of

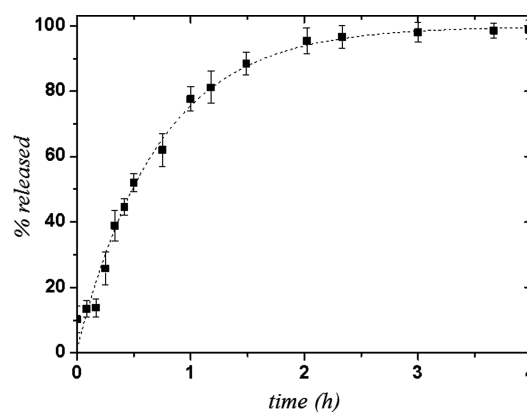


**Figure 8.** Release profile at 25 °C of fluorescein from capsules in contact with ethanol. The dashed line is a guide to the eye only.

silicones in the presence of organic solvents.<sup>31</sup> Thus, the swelled state of the shell enabled the fluorescein molecules to readily diffuse out.

## CONCLUSIONS

A microfluidic device has been used to successfully achieve the one-step production of monodisperse double W/O/W emulsions with a cross-linkable silicone of low viscosity as middle phase. The resulting double emulsion droplets were then used as templates for the formation of capsules via a thermally induced cross-linking reaction of this middle phase. Capsules generated in this way exhibited a mechanical behavior that could be finely tuned by varying the geometric parameters, outer radius and shell thickness, as well as the elastic modulus of the cross-linked network, which depends on the cross-linking time. The systematic generation of silicone capsules with different  $h$  values allowed us to conclude that there is a critical threshold value of  $h$ , below which it is difficult for the shells to retain their spherical shape upon drying. Below this critical  $h$ , capsules buckle and remain buckled after redispersion, unless a cross-linked silicone with a low elastic modulus and large elastic

regime is used. The release of fluorescein from fluorescein-loaded capsules has also been studied over time. The fluorescein release was much faster in thick shells, because of the presence of pores. The release rate also increased when water was replaced by ethanol as receptor solvent, due to the swelling of the capsules. Thus, the present silicone capsules showed solvent-sensitive behavior. Therefore, the present silicone capsules are attractive candidates for molecular delivery purposes, because a vehicle with a predictable and controlled release is a requirement in these applications.

## ■ ASSOCIATED CONTENT

### ● Supporting Information

Plots of the dependence of the outer radius of the emulsion ( $R$ ) on the tip diameter ( $D_{\text{tip}}$ ) and on the flow rate of the outer liquid scaled by the sum of the flow rates of the middle and the inner liquid ( $Q_{\text{OL}}/(Q_{\text{ML}} + Q_{\text{IL}})$ ). Loading and unloading curves of the compression tests performed with silicone monoliths. This material is available free of charge via the Internet at <http://pubs.acs.org>.

## ■ AUTHOR INFORMATION

### Corresponding Author

\*E-mail: [carlos.rodriquez@inl.int](mailto:carlos.rodriquez@inl.int).

### Notes

The authors declare no competing financial interest.

## ■ ACKNOWLEDGMENTS

The authors gratefully acknowledge the Ministerio de Economía y Competitividad (CTQ2011-29336-C03-01), Generalitat de Catalunya (grant 2009-SGR-961), and National Science Foundation (CBET-0967293) for the financial support and A. Manich (IQAC-CSIC) for the help with the characterization of the mechanical properties of the silicone monoliths. C. Rodríguez-Abreu is grateful to the European Union's Seventh Framework Programme (FP7/2007-2013) under Grant 314212, for research funding. N. Vilanova also thanks CSIC for a JAE-predoctoral scholarship.

## ■ REFERENCES

- (1) Kuo, A. C. M. In *Polymer Data Handbook*; Mark, J. E., Ed.; Oxford University Press: New York, 1999; p 411.
- (2) Mark, J. E.; Allcock, H. R.; West, R. *Inorganic Polymers*, 2nd ed.; Oxford University Press: New York, 2005; p 154.
- (3) Mata, A.; Fleischman, A. J.; Roy, S. *Biomedical Devices* **2005**, *7*, 281–293.
- (4) Pina-Hernandez, C.; Kim, J.-S.; Guo, L. J.; Fu, P.-F. *Adv. Mater.* **2007**, *19*, 1222–1227.
- (5) Lu, S.-Y.; Chiu, C.-P.; Huang, H.-Y. *J. Membr. Sci.* **2000**, *176*, 159–167.
- (6) Zielecka, M.; Bujnowska, E. *Prog. Org. Coat.* **2006**, *55*, 160–167.
- (7) Hoefnagels, H. F.; Wu, D.; With, G.; Ming, W. *Langmuir* **2007**, *23*, 13158–13163.
- (8) Liu, Z.; Zhang, X.; Mao, Y.; Zhu, Y. Y.; Yang, Z.; Chan, C. T.; Sheng, P. *Science* **2000**, *289*, 1734–1736.
- (9) Abbasi, F.; Mirzadeh, H.; Katbab, A.-A. *Polym. Int.* **2001**, *50*, 1279–1287.
- (10) Malcolm, R. K.; McCullagh, S. D.; Woolfson, A. D.; Gorman, S. P.; Jones, D. S.; Cuddy, J. J. *Controlled Release* **2004**, *97* (2), 313–320.
- (11) Goller, M. I.; Obey, T. M.; Teare, D. O. H.; Vincent, B.; Wegener, M. R. *Colloids Surf., A* **1997**, *123–124*, 183–193.
- (12) Dufaud, O.; Favre, E.; Sadtler, V. *J. Appl. Polym. Sci.* **2002**, *83*, 967–971.

- (13) Binks, B. P.; Dong, J.; Rebolj, N. *Phys. Chem. Chem. Phys.* **1999**, *1*, 2335–2344.
- (14) Koh, A.; Gillies, G.; Gore, J.; Saunders, B. R. *J. Colloid Interface Sci.* **2000**, *227*, 390–397.
- (15) Jiang, K.; Thomas, P. C.; Forry, A. P.; DeVoe, D. L.; Raghavan, S. R. *Soft Matter* **2012**, *8*, 923–926.
- (16) Ye, C.; Chen, A.; Colombo, P.; Martinez, C. J. *R. Soc. Interface* **2010**, *7*, S461–S473.
- (17) Nie, Z.; Seo, M.; Xu, S.; Lewis, P. C.; Mok, M.; Kumacheva, E.; Whitesides, G. M.; Garstecki, P.; Stone, H. A. *Microfluid. Nanofluid.* **2008**, *5*, 585–594.
- (18) Utada, A. S.; Lorenceau, E.; Link, D. R.; Kaplan, P. D.; Stone, H. A.; Weitz, D. A. *Science* **2005**, *308*, 537–541.
- (19) Utada, A. S.; Fernandez-Nieves, A.; Stone, H. A.; Weitz, D. A. *Phys. Rev. Lett.* **2007**, *99*, 094502.
- (20) Leal-Calderón, F.; Schmitt, V.; Bibette, J. *Emulsion Science. Basic Principles*, 2nd ed.; Springer-Verlag: New York, 2007; p 173.
- (21) Hennequin, Y.; Pannacci, N.; Pulido de Torres, C.; Tetradis-Meris, G.; Chapelot, S.; Bouchaud, E.; Tabeling, P. *Langmuir* **2009**, *25*, 7857–7861.
- (22) Chen, P. W.; Erb, R. M.; Studart, A. R. *Langmuir* **2012**, *28*, 144–152.
- (23) Pogorelov, A. V. *Bending of Surface and Stability of Shells*; American Mathematical Society: Providence, RI, 1988; Vol. 8, p 71.
- (24) Fery, A.; Weinkamer, R. *Polymer* **2007**, *48*, 7221–7235.
- (25) Tsapis, N.; Dufresne, E.; Sinha, S.; Riera, C.; Hutchinson, J.; Mahadevan, L.; Weitz, D. A. *Phys. Rev. Lett.* **2005**, *94*, 018302.
- (26) Zoldesi, C. I.; Imhof, A. *Adv. Mater.* **2005**, *17*, 924–928.
- (27) Gao, C.; Donath, E.; Moya, S.; Dudnik, V.; Mohwald, H. *Eur. Phys. J. E.* **2001**, *5*, 21–27.
- (28) He, W.-D.; Zou, Y.-F.; Pan, C.-Y. *J. Appl. Polym. Sci.* **1998**, *69*, 619–625.
- (29) Yow, H. N.; Routh, A. F. *Langmuir* **2009**, *25*, 159–166.
- (30) Song, Y.; Srinivasarao, M.; Tonelli, A.; Balik, C. M.; McGregor, R. *Macromolecules* **2000**, *33*, 4478–4485.
- (31) Yoo, S. H.; Cohen, C.; Hui, C.-Y. *Polymer* **2006**, *47*, 6226–6235.